Tyrosine Phosphorylation of the *vav* Proto-Oncogene Product in Activated B Cells

Xosé R. Bustelo and Mariano Barbacid

Activation of B lymphocytes by engagement of their immunoglobulin M antigen receptors results in phosphorylation of a number of proteins on tyrosine residues. One such protein is p95^{vav}, the product of the *vav* proto-oncogene. Tyrosine phosphorylation of p95^{vav} occurred within seconds of immunoglobulin M cross-linking and was independent of other events induced during stimulation of B cells, such as protein kinase C activation, guanosine triphosphate–binding protein signaling, and calcium mobilization. Moreover, engagement of antigen receptors induced the rapid (~5 seconds) and transient (~60 seconds) association of p95^{vav} with a 70-kilodalton tyrosine-phosphorylated protein, Vap-1, an interaction mediated by the Src homology 2 domain of p95^{vav}. These results suggest that the *vav* proto-oncogene participates in the signaling processes that mediate the antigen-induced activation of B lymphocytes.

Many substrates of tyrosine protein kinases contain a structural domain, the Src homology 2 (SH2) region, that mediates their interaction with activated tyrosine protein kinases, presumably by binding to phosphotyrosine residues (*1*). A recently identified SH2-containing protein is p95^{vav}, the product of the *vav* proto-oncogene, a locus that is expressed only in cells of hematopoietic origin (*2*). The p95^{vav} protein also has an intriguing array of other structural motifs. The NH_2-terminal moiety of p95^{vav} contains helix-loop-helix (HLH) and leucine zipper–like domains that have limited similarity to motifs located at the COOH-terminus of proteins of the Myc family. Deletion of the HLH motif of p95^{vav} results in its oncogenic activation (*3*, *4*). The p95^{vav} protein contains a zinc finger–like domain reminiscent of the phorbol ester–binding region of protein kinase C, diacylglycerol kinase, and the c-Raf oncoprotein and two SH3 regions flanking the SH2 domain (*1*, *3*). Finally, p95^{vav} has a region of similarity with the product of the *dbl* proto-oncogene, the yeast CDC24 GDP-GTP (guanosine diphosphate–guanosine triphosphate) exchange factor, and the *brc* gene (*5*). The p95^{vav} protein becomes phosphorylated on tyrosine residues in T cells after activation of the T cell receptor–CD4 complex and in mast cells after engagement of their FcεRI high-affinity immunoglobulin E (IgE) receptors (*6*). These findings led us to investigate whether p95^{vav} might participate in B cell signaling processes mediated by tyrosine protein kinases.

The immature WEHI-231 and the mature Bal17 B cell lines were selected for this study (*7*). These cell lines express similar amounts of p95^{vav} as determined by immunoprecipitation of the protein from extracts of ^{35}S-labeled cells with antibodies to a synthetic p95^{vav} peptide (anti-Vav) (Fig. 1) (*8*). One of the most immediate biochemical responses detected after IgM antigen receptor engagement is the induction of protein phosphorylation on tyrosine residues (*9*, *10*). Unstimulated WEHI-231 and Bal17 cells had very low amounts of tyrosine-phosphorylated proteins as determined by immunoblot analysis of proteins from cell extracts with antibodies to phosphotyrosine (Fig. 2A). However, addition of antibodies to IgM heavy chain (anti-μ) to either of these B cell lines elicited an increase in the tyrosyl phosphorylation of more than ten different proteins within 5 s (Fig. 2A).

Proteins from WEHI-231 and Bal17 cell lines and from splenic B lymphocytes were blotted with anti-Vav to determine the amount of p95^{vav} present during B cell activation. The amount of p95^{vav} in these cells was not affected by engagement of surface IgM (Fig. 2B). In contrast, phosphorylation of p95^{vav} on tyrosine residues was increased within 5 s after cross-linking of IgM antigen receptor with anti-μ (Fig. 2C). Tyrosine phosphorylation of p95^{vav} was maximal within 15 to 30 s and declined thereafter. Quantitative densitometric analysis indicated that tyrosine phosphorylation of p95^{vav} increased 12.6-fold in Bal17 cells and 8-fold in WEH1-231 cells after cross-linking of IgM. Induction of tyrosine phosphorylation of p95^{vav} also occurred in normal splenic mouse B lymphocytes (Fig. 2C).

To determine whether p95^{vav} became phosphorylated on serine or threonine residues as a consequence of B cell activation, we labeled WEHI-231 cells with [^{32}P]orthophosphate and examined the phosphoamino acid content of p95^{vav} before and after the cells were incubated for 5 min with anti-μ. The p95^{vav} in unstimulated WEHI-231 cells contained detectable amounts of phosphotyrosine and phosphoserine. After incubation of cells with anti-μ only the amount of phosphotyrosine residues was increased (Fig. 3).

The rapid kinetics of tyrosine phosphorylation of p95^{vav} after cross-linking of surface IgM suggests that this biochemical event may be the direct consequence of the activation of one or more tyrosine protein kinases by the IgM antigen receptors. We therefore studied the effects of various pharmacological agents on tyrosine phosphorylation of p95^{vav} in WEHI-231 cells. Incubation of these cells with sodium vanadate had no effect on tyrosine phosphorylation of p95^{vav}, indicating that the increased incorporation of ^{32}P observed after cross-linking of IgM was probably due to the activation of one or more tyrosine kinases and not to inactivation of a tyrosine phosphatase. Similarly, treatment of WEHI-231 cells with aluminum fluoride for up to 60 min did not affect tyrosine phosphorylation of p95^{vav}, indicating that activation of tyrosine phosphorylation is not mediated by a heterotrimeric GTP-binding protein (G protein).

Treatment of WEHI-231 cells with tumor promoters and Ca^{2+} ionophores mim-

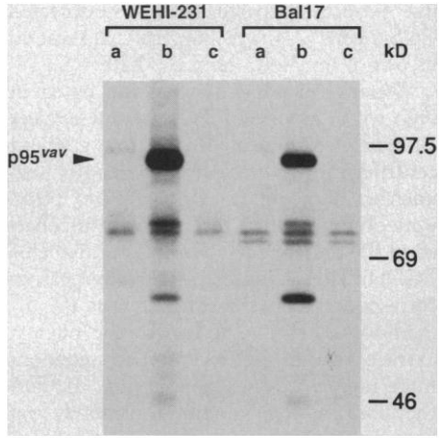

Fig. 1. Expression of the *vav* proto-oncogene in murine lymphoid B cell lines. WEHI-231 and Bal17 cells (5×10^7) were metabolically labeled with a mixture of [^{35}S]methionine and [^{35}S]cysteine (trans-[^{35}S]label, 50 μCi/ml, ICN Biochemicals) for 3 hours. Labeled cells were collected by centrifugation and suspended in 1× RIPA buffer [10 mM tris-HCl (pH 8.0), 150 mM NaCl, Triton X-100 (1%), aprotinin (1%) (Sigma), and 250 μM phenylmethylsulfonyl fluoride]. Lysates were centrifuged and supernatants incubated with (a) preimmune serum or (b and c) immune serum to a peptide corresponding to mouse p95^{vav} sequences (*8*) either in the (b) absence or (c) presence of competing peptide (20 μg/ml). The resulting immunoprecipitates were analyzed by 8% SDS–polyacrylamide gel electrophoresis (PAGE). The migration of p95^{vav} is indicated by an arrowhead. Molecular size markers included phosphorylase b (97.5 kD), albumin (69 kD), and ovoalbumin (46 kD).

Department of Molecular Biology, Bristol-Myers Squibb Pharmaceutical Research Institute, Princeton, NJ 08543–4000.

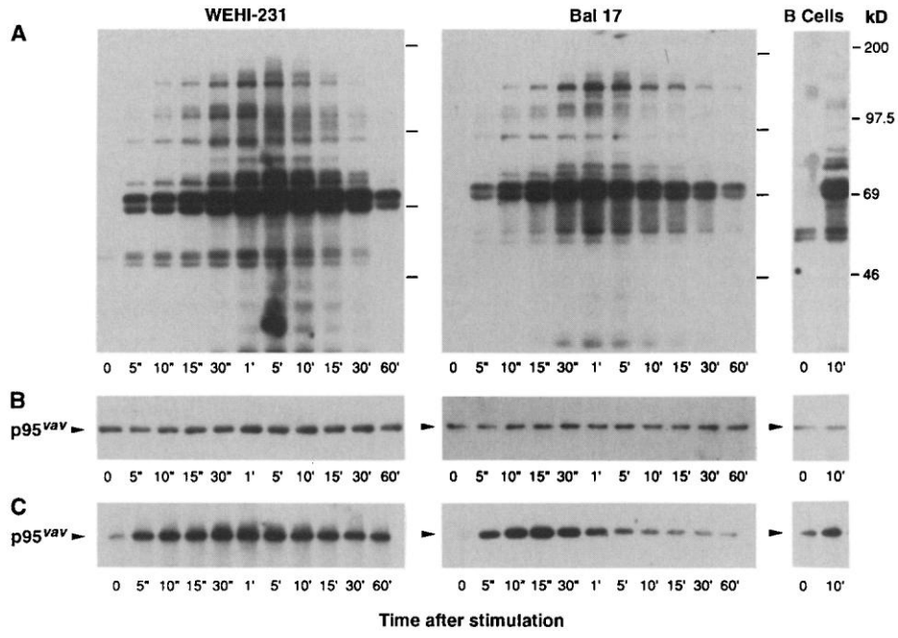

Fig. 2. Phosphorylation of p95^{vav} on tyrosine residues in B cells stimulated with antibodies to IgM. WEHI-231 and Bal17 cells were stimulated for the indicated times with affinity-purified goat antibodies (30 μg/ml) to the μ chain of IgM (anti-μ) (Sigma). Murine splenic B lymphocytes were selected by removal of T cells with monoclonal antibodies to Thy-1 (*15*) and stimulated with anti-μ (10 μg/ml). Stimulation was terminated by addition into the medium of 1/5 volume of 5× RIPA buffer containing NaF (2.5 mM) and sodium orthovanadate (500 μM). (**A**) Tyrosine-phosphorylated proteins in total cell extracts. Lysates derived from 5 × 10^5 cells were diluted with one volume of 2× SDS-PAGE sample buffer [160 mM tris-HCl (pH 6.8), SDS (4%), glycerol (20%), β-mercaptoethanol (1%), and bromophenol blue (0.04%)], boiled, and fractionated by SDS-PAGE (8% gels). Proteins were transferred onto nitrocellulose filters (Schleicher & Schuell) with a semidry apparatus (Millipore) and identified by protein immunoblot analysis with monoclonal antibodies to phosphotyrosine (4G10, Upstate Biotechnology) as described (*6*). (**B**) Quantitative analysis of the amount of p95^{vav} present in each lane. Lysates from cells (2 × 10^6) were processed as in (A) and blotted with antibodies to an MBP fusion protein containing the zinc finger–like domain of p95^{vav} (*8*). (**C**) Phosphorylation of p95^{vav} on tyrosine residues during stimulation of B cells. Lysates from 2 × 10^7 cells were incubated with the antibodies to Vav described in (B). The resulting immunoprecipitates were fractionated by SDS-PAGE (8% gels) and analyzed by protein immunoblotting with antibodies to phosphotyrosine. The migration of p95^{vav} is indicated by solid arrowheads. Molecular size markers included myosin (200 kD), phosphorylase b (97.5 kD), albumin (69 kD), and ovoalbumin (46 kD).

ics their activation through antigen-stimulated receptors. Addition of either the tumor promotor phorbol 12-myristate-13-acetate (PMA) (50 ng/ml) or the Ca^{2+} ionophore ionomycin (60 to 500 nM) or both to WEHI-231 cells had no effect on tyrosine phosphorylation of p95^{vav}. These results suggest that tyrosine phosphorylation of p95^{vav} may occur earlier in the signaling pathway than the hydrolysis of phosphatidylinositol 4,5-bisphosphate (PIP_2), which is presumably bypassed by the addition of PMA (which activates protein kinase C) and ionomycin (which increases intracellular Ca^{2+}). Alternatively, p95^{vav} may be part of an independent signal transduction pathway also required for activation of B cells.

We searched for proteins that might become associated with p95^{vav} after engagement of the cell surface IgM. When extracts from WEHI-231 cells stimulated with anti-μ were incubated with anti-Vav in the presence of nonionic detergents, a 70-kD tyrosine-phosphorylated polypeptide was co-immunoprecipitated with p95^{vav} (Fig. 4A). This polypeptide, designated Vap-1 (*V*av-*a*ssociated *p*rotein), was not detected when we preincubated the immune serum with the immunizing peptide (Fig. 4A). Vap-1 was also detected on immunoblots of proteins immunoprecipitated with two other antisera to bacterially synthesized p95^{vav} sequences fused to the maltose binding protein (MBP). These p95^{vav} sequences include those encompassing the cysteine-rich zinc finger–like region and the HLH–leucine zipper domain (*8*) (Fig. 4A). Concentrations of SDS as high as 0.3% had no effect on the recognition of p95^{vav} by these antibodies. However, the presence of Vap-1 in these immunoprecipitates was completely inhibited by low concentrations (0.1%) of SDS (Fig. 4B). Similar results were obtained with Bal17 cells. These observations suggest that the presence of the tyrosine-phosphorylated Vap-1 in p95^{vav} immunoprecipitates is due to a physical association between these two proteins.

SH2 domains may mediate protein-protein interactions by binding to phosphotyrosine residues (*1*). Therefore, we investigated whether the association between p95^{vav} and Vap-1 might be mediated by the SH2 domain of p95^{vav}. Extracts of nonstimulated and stimulated WEHI-231 cells were incubated with a bacterial MBP fusion protein containing the entire p95^{vav} SH2 domain (*11*), and proteins that bound to the fusion protein were detected by immunoblotting with antibodies to phosphotyrosine. The bacterial MBP-VavSH2 fusion protein bound a protein of the same molecular size as Vap-1 which we assume is Vap-1. No other phosphotyrosine-containing proteins, including p95^{vav}, could be identified in these complexes. Addition of free phosphotyro-

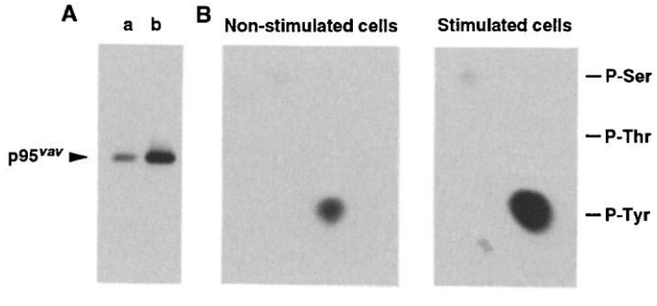

Fig. 3. Phosphoamino acid analysis of p95^{vav} in activated B cells. (**A**) WEHI-231 cells were labeled in vivo for 3.5 hours with [^{32}P]orthophosphoric acid (0.5 mCi/ml, Amersham) and either (a) not stimulated or (b) stimulated by incubation for 5 min with anti-μ (30 μg/ml). Cells were lysed in 1× RIPA buffer containing NaF (1 mm) and sodium orthovanadate (100 μM), immunoprecipitated with antibodies to a synthetic peptide corresponding to a portion of Vav (*8*), and analyzed by SDS-PAGE (8% gels). The migration of p95^{vav} is indicated by an arrowhead. (**B**) Phosphoamino acid analysis of ^{32}P-labeled p95^{vav}. The samples described in (A) were transferred to Immobilon-P membranes (Millipore) with a semidry blotting apparatus. Those regions of the membrane containing p95^{vav} were excised, incubated with HCl for 1 hour at 110°C, and analyzed by two-dimensional thin-layer chromatography as described (*6*). The migration of the phosphoamino acid standards phosphoserine (P-Ser), phosphothreonine (P-Thr), and phosphotyrosine (P-Tyr) is indicated.

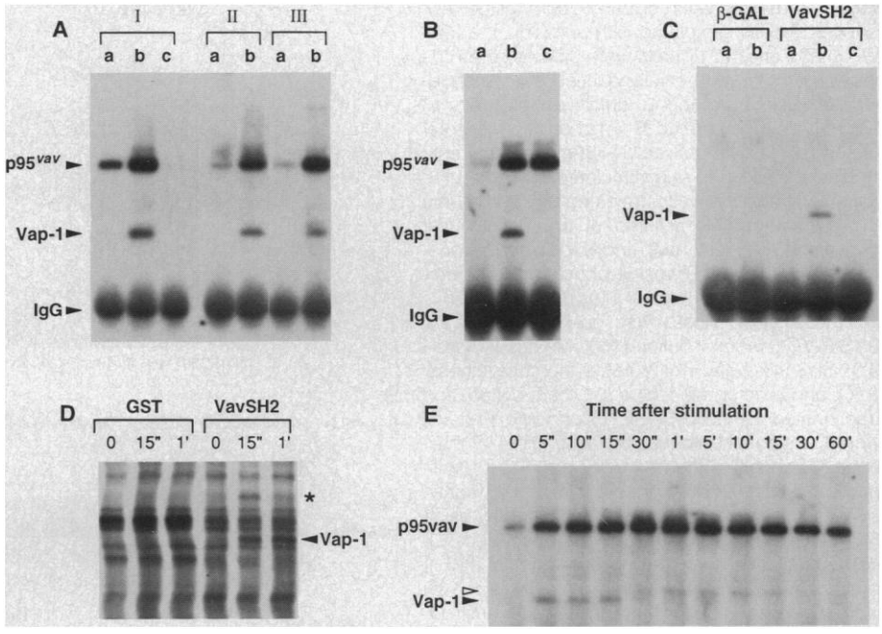

Fig. 4. Association of p95^{vav} with a 70-kD tyrosine-phosphorylated protein (Vap-1). (**A**) Identification of tyrosine-phosphorylated Vap-1 in p95^{vav} immunoprecipitates obtained from WEHI-231 cells (2 × 10^7) stimulated for 15 s with anti-μ (30 μg/ml) with three independent antisera to Vav raised against (I) a p95^{vav} peptide, (II) an MBP-Vav zinc finger fusion protein, and (III) an MBP-Vav HLH fusion protein (*8*). Unstimulated (a) or stimulated (b and c) cells were incubated with antibodies to Vav either in the absence (a and b) or presence (c) of competing peptide (20 μg/ml). Immunoprecipitated proteins were separated by SDS-PAGE (8% gels) and analyzed by protein immunoblotting with antibodies to phosphotyrosine. (**B**) Inhibition of the association of Vap-1 with p95^{vav} by SDS. Unstimulated (a) or stimulated (b and c) WEHI-231 cells (2 × 10^7) were incubated with antibodies to the MBP-Vav zinc finger fusion protein either in the absence (a and b) or presence (c) of SDS (0.3%). The immunoprecipitated proteins were separated by SDS-PAGE (8% gels) and analyzed by protein immunoblotting with antibodies to phosphotyrosine. (**C**) Binding of tyrosine-phosphorylated Vap-1 to the SH2 domain of p95^{vav}. Cell lysates derived from WEHI-231 cells (2 × 10^7) either not stimulated (a) or stimulated (b and c) for 15 s with anti-μ (30 μg/ml) were incubated for 3 hours at 4°C with either an MBP–β-galactosidase fusion protein (β-GAL) or with the MBP-VavSH2 fusion protein (VavSH2) bound to Sepharose beads (*11*) in the absence (b) or presence (c) of free phosphotyrosine (30 mM). Bound proteins were eluted and analyzed by protein immunoblotting with antibodies to phosphotyrosine. (**D**) Association of Vap-1 with the p95^{vav} SH2 domain after B cell activation. ^{35}S-labeled WEH1-231 cells (2 × 10^7) were either not stimulated or stimulated with anti-μ for the indicated periods of time and lysed with 5× RIPA buffer containing phosphatase inhibitors. Cellular lysates were then incubated with either glutathione S-transferase protein (GST) alone or with a GST-VavSH2 fusion protein (VavSH2) bound to glutathione-Sepharose beads (*11*). Bound proteins were analyzed by SDS-PAGE (8% gels). (**E**) Kinetic analysis of the association between Vap-1 and p95^{vav}. WEHI-231 cells (2 × 10^7) were stimulated with anti-μ (30 μg/ml) for the indicated times, lysed with 5× RIPA buffer containing phosphatase inhibitors, and incubated with antibodies to the MBP-Vav zinc finger fusion protein (*8*). Immunoprecipitates were fractionated by SDS-PAGE (8% gels) and immunoblotted with antibodies to phosphotyrosine. (A through E) The migrations of p95^{vav}, Vap-1, and the Ig heavy chain (IgG) are indicated by solid arrows. (D) The migration of an 83-kD protein occasionally associated with the GST-VavSH2 fusion protein in stimulated B cells is indicated by an asterisk. (E) An open arrowhead indicates the migration of a 75-kD protein recognized by antibodies to the bacterial moiety of the MBP-Vav zinc finger fusion protein (*8*).

sine (30 mM) partially inhibited the interaction of Vap-1 with the MBP-VavSH2 fusion protein (Fig. 4C). Similar results were obtained with a glutathione S-transferase (GST) VavSH2 fusion protein (*11*), thus indicating that the interaction of Vap-1 with p95^{vav} is mediated by its SH2 domain.

Incubation of the GST-VavSH2 fusion protein with extracts from ^{35}S-labeled WEHI-231 cells revealed that Vap-1 associated with the SH2 domain of p95^{vav} only after IgM cross-linking (Fig. 4D). The bacterial GST protein alone did not associate with Vap-1. These results indicate that the formation of the p95^{vav}/Vap-1 complex is a direct consequence of B cell activation. Subsequent kinetic studies showed that p95^{vav} associates with tyrosine-phosphorylated Vap-1 as early as 5 s after cross-linking of IgM (Fig. 4E). These results suggest that the association between p95^{vav} and Vap-1 may require their phosphorylation on tyrosine residues.

Vap-1 was no longer present in p95^{vav} immunoprecipitates generated 1 min after cross-linking of the surface IgM (Fig. 4E). Because these experiments were conducted in the presence of sodium vanadate, the absence of detectable Vap-1 protein in these immunoprecipitates is probably due to its dissociation from p95^{vav} rather than to dephosphorylation of its tyrosine residues. This interpretation is further supported by the presence of Vap-1 in MBP-VavSH2 complexes even 10 min after IgM cross-linking. These findings suggest that p95^{vav} may interact with a third protein that facilitates its rapid dissociation from Vap-1.

Normal B lymphocytes express three members of the *src* gene family of kinases, p56^{blk}, p56^{lyn} and p60^{fyn}, whereas WEHI-231 cells contain at least p56^{lyn} (*12*). These kinases are associated with surface IgM and IgD and their catalytic activity is stimulated by binding of antigen to these receptors or by cross-linking of the receptors with antibodies (*12*). Moreover, WEHI-231 and normal B lymphocytes contain at least two other tyrosine kinases of 72 kD and 80 kD whose relationship with the *src* family of kinases remains to be established (*10, 13*). The rapid rate of tyrosine phosphorylation of p95^{vav} during B cell activation suggests that this protein may be a substrate of one or more tyrosine protein kinases associated with the IgM antigen receptor complex. Neither immunoprecipitates containing p95^{vav} nor the MBP-VavSH2 fusion complexes containing the Vap-1 protein have detectable tyrosine protein kinase activity (*14*). These observations suggest that the association between p95^{vav} and its tyrosine kinase might be very transient and may not involve the formation of stable complexes like those described for cell surface tyrosine protein kinase receptors and their respective substrates (*1*). Alternatively, p95^{vav} might be a substrate for a different class of tyrosine protein kinases whose requirements for in vitro kinase activity remain to be determined.

REFERENCES AND NOTES

1. C. A. Koch, D. Anderson, M. F. Moran, C. Ellis, T. Pawson, *Science* **252**, 668 (1991).
2. S. Katzav, D. Martin-Zanca, M. Barbacid, *EMBO J.* **8**, 2283 (1989).
3. J. Coppola, S. Bryant, T. Koda, D. Conway, M. Barbacid, *Cell Growth Differ.* **2**, 95 (1991).
4. S. Katzav, J. L. Cleveland, H. E. Heslop, D. Pulido, *Mol. Cell. Biol.* **11**, 1912 (1991).
5. F. Galland, S. Katzav, D. Birnbaum, *Oncogene* **7**, 585 (1992); J. M. Adams, H. Houston, J. Allen, T. Lints, R. Harvey, *ibid.*, in press.
6. X. R. Bustelo, J. A. Ledbetter, M. Barbacid, *Nature* **356**, 68 (1992); B. Margolis *et al.*, *ibid.*, p. 71.
7. J. Mizuguchi, W. Tsang, S. L. Morrison, M. A. Beave, W. E. Paul, *J. Immunol.* **137**, 2162 (1986); J. Mizuguchi, M. A. Beaven, J. Hu-Li, W. E. Paul, *Proc. Natl. Acad. Sci. U.S.A.* **83**, 4474 (1986); J.

Mizuguchi, N. Utsonomiya, M. Nakanishi, Y. Arata, *J. Immunol.* **140**, 2495 (1988).
8. The rabbit polyclonal antibodies to Vav used in this study include antibodies to a synthetic peptide corresponding to residues 576 to 589 of mouse $p95^{vav}$, a bacterial MBP fusion protein containing the cysteine-rich zinc finger–like region of mouse $p95^{vav}$ (residues 460 to 626), and a bacterial MBP fusion protein containing the HLH–leucine-rich region of mouse $p95^{vav}$ (residues 9 to 135).
9. M. R. Gold, D. A. Law, A. L. DeFranco, *Nature* **345**, 810 (1990); M. Brunswick, L. E. Samelson, J. J. Mond, *Proc. Natl. Acad. Sci. U.S.A.* **88**, 1311 (1991).
10. M. A. Campbell and B. M. Sefton, *EMBO J.* **9**, 2125 (1990).
11. Sequences encoding the murine $p95^{vav}$ SH2 domain (residues 659 to 773) were amplified by the polymerase chain reaction (PCR) with the pJC11 plasmid (*3*) as template and subcloned into the pMAL-c (NE Biolabs) or the pGEX-2T (Pharmacia) expression vectors. Cultures of *Escherichia coli* DHα cells transformed with pMAL-c expression plasmids containing the MBP fused to either the LacZ gene (β-gal) or the SH2 domain of $p95^{vav}$ were processed as suggested by the manufacturer. The MBP fusion proteins were purified by affinity chromatography with an amylose matrix and eluted in RIPA buffer containing maltose (10 mM). After elution, fusion proteins were immobilized on protein A–Sepharose beads (Pharmacia) coated with antibodies to MBP (NE Biolabs). Cultures of *E. coli* DHα containing the pGEX-2T plasmid encoding either the glutathione S-transferase (GST) protein alone or the GST-VavSH2 fusion protein were induced following standard protocols, and expressed proteins were purified with glutathione-Sepharose beads (Pharmacia). These beads were incubated directly with cellular lysates. In binding experiments, cells were lysed by adding into the medium 1/5 volume of 5× RIPA buffer containing phosphatase inhibitors. Lysates were mixed with Sepharose beads containing the appropriate bacterial MBP fusion protein by gentle inversion for 3 hours at 4°C. Complexes were recovered by centrifugation, washed, and eluted with SDS-PAGE sample buffer.
12. Y. Yamanashi, T. Kakiuchi, J. Mizuguchi, T. Yamamoto, K. Toyoshima, *Science* **251**, 192 (1991); A. L. Burkhardt, M. Brunswick, J. B. Bolen, J. J. Mond, *Proc. Natl. Acad. Sci. U.S.A.* **88**, 7410 (1991).
13. J. E. Hutchcroft, M. L. Harrison, R. L. Geahlen, *J. Biol. Chem.* **266**, 14846 (1991).
14. X. R. Bustelo and M. Barbacid, unpublished observations.
15. J. E. Coligan, A. M. Kruisbeek, D. H. Margulies, E. M. Shevach, W. Strouber, *Current Protocols in Immunology* (Wiley Interscience, New York, 1991), chap. 3.
16. We thank A. Burkhardt and J. Bolen for providing the WEHI-231 and Bal17 B cell lines and K. L. Suen for generating the plasmid encoding the GST-VavSH2 fusion protein. X.R.B. was supported by a postdoctoral fellowship from the Spanish Ministerio de Educación y Ciencia.

29 January 1992; accepted 16 April 1992

Calmodulin Trapping by Calcium-Calmodulin–Dependent Protein Kinase

Tobias Meyer,* Phyllis I. Hanson, Lubert Stryer, Howard Schulman†

Multifunctional calcium-calmodulin–dependent protein kinase (CaM kinase) transduces transient elevations in intracellular calcium into changes in the phosphorylation state and activity of target proteins. By fluorescence emission anisotropy, the affinity of CaM kinase for dansylated calmodulin was measured and found to increase 1000 times after autophosphorylation of the threonine at position 286 of the protein. Autophosphorylation markedly slowed the release of bound calcium-calmodulin; the release time increased from less than a second to several hundred seconds. In essence, calmodulin is trapped by autophosphorylation. The shift in affinity does not occur in a site-directed mutant in which threonine at position 286 has been replaced by a non-phosphorylatable amino acid. These experiments demonstrate the existence of a new state in which calmodulin is bound to CaM kinase even though the concentration of calcium is basal. Calmodulin trapping provides for molecular potentiation of calcium transients and may enable detection of their frequency.

Multifunctional CaM kinase is a ubiquitous mediator of Ca^{2+} effects in neurotransmission, neuronal plasticity, ion channels, and carbohydrate metabolism (*1*). CaM kinase constitutes up to 1% of total brain protein and 2% of hippocampal protein, and its concentration in synaptic spines is roughly comparable to that of total calmodulin (*2*). Neuronal CaM kinase consists of α (54 kD) and β or β′ (60 or 58 kD) subunits in ~10 subunit multimers. Each isoform has a catalytic domain, a regulatory domain consisting of an autoinhibitory and a calmodulin-binding region, and an association (oligomerization) domain. Each subunit of the kinase becomes activated when Ca^{2+}-calmodulin binds to and displaces the autoinhibitory domain from its active site. The activated kinase further disrupts the interaction of the autoinhibitory region with the catalytic site by phosphorylating Thr^{286} and Thr^{287} of the α and β subunits, respectively. After dissociation of calmodulin from an autophosphorylated CaM kinase, the modified subunit remains partially active (termed autonomous). Subsequent Ca^{2+}-independent autophosphorylation occurs within the vacated calmodulin-binding region; these phosphorylated residues are termed inhibitory sites because their modification blocks the binding of calmodulin and thereby prevents maximal activation.

We have investigated the effect of autophosphorylation of CaM kinase on binding and release of calmodulin by the technique of fluorescence emission anisotropy (*3*) with dansylated calmodulin (CaM^F) as a probe (*4*). The rotational mobility of CaM^F can be assessed by exciting with vertically polarized light and measuring differences in emission of vertically (F_V) and horizontally (F_H) polarized light. The emission anisotropy is defined as $A = (F_V - F_H)/(F_V + 2F_H)$. The value of A increases when calmodulin (17 kD) binds to CaM kinase (~600 kD) because the rotational mobility of the fluorescent probe is markedly decreased. The binding of Ca^{2+} to CaM^F in the absence of CaM kinase resulted in a small decrease in anisotropy (Fig. 1). Subsequent addition of purified rat brain CaM kinase (*5*) in the absence of adenosine triphosphate (ATP) led to a large increase

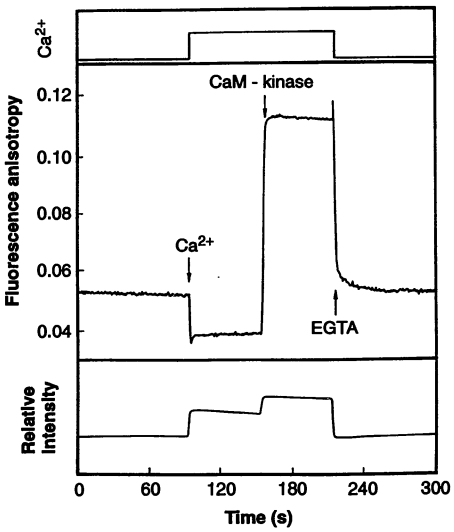

Fig. 1. Time course of binding and release of dansylated CaM from CaM kinase. The buffer solution contained 5 mM Mg^{2+}, 50 mM potassium acetate, and 15 mM Hepes (pH 7, adjusted with KOH). Increasing the free Ca^{2+} concentration from 100 nM to 200 μM decreases the fluorescence anisotropy of CaM^F (20 nM) slightly from 0.054 to 0.040. Addition of an excess of CaM kinase (60 nM binding sites) markedly increases the fluorescence anisotropy to 0.12. This increase is due to the binding of CaM^F to the large CaM kinase oligomer. When the free Ca^{2+} concentration is lowered to less than 100 nM by addition of 3 mM EGTA, the fluorescence anisotropy drops rapidly to 0.054, the value characteristic of free CaM^F without bound Ca^{2+}.

T. Meyer and L. Stryer, Department of Cell Biology, Stanford University School of Medicine, Stanford, CA 94305.
P. I. Hanson and H. Schulman, Department of Pharmacology, Stanford University School of Medicine, Stanford, CA 94305.

*Present address: Department of Cell Biology, Duke University Medical Center, Durham, NC 27710.
†To whom correspondence should be addressed.